Neurobiology of Aging 103 (2021) 42–51

Contents lists available at ScienceDirect

Neurobiology of Aging

journal homepage: www.elsevier.com/locate/neuaging.org

Regular Article

Age, sex, and cerebral microbleeds in EFAD Alzheimer disease mice

Mafalda Cacciottolo[a], Todd E. Morgan[a], Caleb E. Finch[a,b,*]

[a] Leonard Davis School of Gerontology, University of Southern California, Los Angeles, CA, USA
[b] Departments of Neurobiology and Molecular Biology, The Dornsife College, University of Southern California, Los Angeles, CA, USA

ARTICLE INFO

Article history:
Received 12 December 2020
Revised 23 February 2021
Accepted 23 February 2021
Available online 28 February 2021

Keywords:
Alzheimer's disease (AD)
Amyloid β-peptide (Aβ)
Apolipoprotein E (APOE)
Cerebral amyloid angiopathy (CAA)
EFAD mice
Microbleeds (MBs)
Blood pressure

ABSTRACT

Cerebral microbleeds (MBs) increase at later ages in association with increased cognitive decline and Alzheimer Disease (AD). MB prevalence is also increased by APOE4 and hypertension. In EFAD mice (5XFAD$^{+/-}$/human APOE$^{+/+}$), cerebral cortex MBs are most prevalent in E4 females at 6 months, paralleling plaque amyloid. We evaluated MBs at 2, 4, and 6 months in relation to amyloid in plaques and cerebral amyloid angiopathy (CAA) by age, sex, APOE allele, and blood pressure. At 2 mo, MBs were 50% more numerous than plaques, followed by decreased ratio of MBs:Aβ plaques with female excess to 6 mo. The stable size of MBs suggests MBs arise as single events of extravasation, which may "seed" plaque formation. Blood pressure was normal from 2 to 6 months, minimizing a role of hypertension. Memory, assessed by fear conditioning, decreased with age in correlation with MBs and amyloid. Cortical layer analysis showed prevalent MBs and plaque in layers 4 and 5. Contrarily, CAA was prevalent in layers 1 and 2, discounting its contribution to MBs.

1. Introduction

Cerebral microbleeds (MBs) are punctate blood residues identified by MRI as hypointense lesions within the brain parenchyma with a diameter <10 mm (Greenberg et al. 2009; Gregoire et al. 2009; Wardlaw et al. 2013). MBs are associated with cerebrovascular disease and hypertension (Poels et al. 2010; Jia et al. 2014; Blevins et al. 2020; Petrea et al. 2020), and Alzheimer's disease (AD) (Akoudad et al. 2016; Charidimou et al. 2018). In a MRI and PET-based study from the Mayo Clinic, MBs increased with age by >5-fold between age 50 and 90, with male excess, in proportion to cortical amyloid (Graff-Radford et al. 2020). However, in an autopsy series with parallel histological analysis, smaller MBs were underestimated by MRI (Haller et al. 2019).

Besides age, APOE4 is a major MB risk factor (Yates et al. 2014; Cacciottolo et al. 2016; Knol et al. 2020; Li et al. 2020). The APOE4 impact on MBs is increased by hypertension (Shi et al. 2018; Biffi et al. 2019). The 50% excess of MBs in males from different clinical cohorts was also increased by APOE4 (Cacciottolo et al. 2016). In mice with human AD transgenes, MBs are increased by APOE4 (Bell et al. 2012; Cacciottolo et al. 2016) and by hypertension (Nyul-Toth et al. 2020). APOE also enhances blood-brain barrier leakage with aging and AD (Montagne et al. 2020).

The origins of MBs remain unclear. The frequent concurrence of MBs with cerebral amyloid angiopathy (CAA) in AD suggested that MBs are extravasation from weakened CAA vessel walls (Fisher 2014; Charidimou et al. 2018). This hypothesis is challenged by the limited co-localization of MBs with CAA (Bell et al. 2012; van Veluw et al. 2017; van Veluw et al. 2020). A direct relationship of MBs to amyloid plaques is indicated by 3 lines of evidence (1) MBs were colocalized within extracellular amyloid in an FAD mouse (Tanifum et al. 2014); (2) laser-induced occlusion of single capillaries in APP/PSI mice caused rapidly increased fibrillar amyloid (Zhang et al. 2019); (3) rapid amyloid deposition around trace bleeds was induced by needle tracks in wild-type rodents (Chuang et al. 2012; Purushothuman et al. 2013).

To further resolve the relationships of MBs to plaque and vascular amyloid, we examined EFAD mice for the time course of occurrence. EFAD mice carry transgenes for five familial dominant AD genes in combination with human APOE3 and APOE4 alleles (5XFAD$^{+/-}$ /human APOE$^{+/+}$) (Youmans et al. 2012). At age 6 months, female E4FAD mice had the most brain amyloid accumulation and 3-5-fold excess of MBs (Cacciottolo et al. 2016). The majority of MBs were associated with amyloid plaques; a modest female excess of CAA (50%) was restricted to E3FAD. Two hypotheses for MBs are considered: MBs arise by leakage from the amyloid containing cerebral blood vessels (CAA). Alternatively, MBs arise

* Corresponding author at: Leonard Davis School of Gerontology, 3715 McClintock Ave, University of Southern California, Los Angeles, CA 90089-0191, USA. Tel. 213 740 4915; fax: 213 740 0792.
E-mail address: cefinch@usc.edu (C.E. Finch).

0197-4580/$ – see front matter © 2021 Elsevier Inc. All rights reserved.
https://doi.org/10.1016/j.neurobiolaging.2021.02.020

from the encroachment of extracellular amyloid plaque. These hypotheses were addressed by examining the time course, size and localization of MBs in relation to CAA and plaque in cortical layers by sex and APOE for ages 2–6 months.

Microglia were analyzed for colocalization with MBs because microglial processes rapidly respond to extracellular iron deposits (Fisher et al. 2010; Gong et al. 2019). We also evaluated the possible role of blood pressure, which increases by 6 mo in C57BL/6 female mice (Keller et al. 2019), while cerebral arteries become more rigid at later ages (Liu et al. 2012; Diaz-Otero et al. 2016). EFAD mice have not been studied for blood pressure. Fear conditioned learning assessed cognitive decline in relation to MBs, amyloid, and CAA.

2. Material and methods

2.1. Animals

All procedures were approved by the University of Southern California Institutional Animal Care and Use Committee (USC IACUC, protocol 20417), supervised by the USC Department of Animal Resources. EFAD mice (5XFAD$^{+/-}$ /human APOE$^{+/+}$) were generously provided by Professor Mary Jo LaDu, Univ. Illinois at Chicago) and genotyped (Youmans et al. 2012)). Mice were fed ad libitum Purina Lab Chow (LabDiet, Hayward, CA) and sterile water; housed in groups of 5 at 22°C/30% humidity and light cycles of 0600–1800 hours with standard nesting material; and allowed free movement. A total of 8 groups (5–10 mice per group, both sexes and APOE3 & -4 alleles) were examined at 2, 4, and 6 months.

2.2. Tissues

Mice were euthanized by isoflurane, perfused transcardially with PBS and brains collected. Hemisected brains were fixed in 4% paraformaldehyde and cryoprotected in 0.003% sodium azide for sagittal Vibratome sectioning 0.5–2 mm from midline. The other hemisphere was dissected and stored at −80 °C. All assays used observer-blinded protocols.

2.3. Microbleeds

Extracellular hemosiderin was analyzed in cerebral cortex by Prussian blue histochemistry, which detects extravasated heme ferric iron in ferritin and hemosiderin complexes (Sullivan et al. 2008; Cacciottolo et al. 2016). Sections (40 µm, spaced 400 µm, 5 sections per mouse) were counterstained by nuclear fast red (Sigma-Aldrich). Hemosiderin deposits were individually analyzed for numbers of puncta per brain section, averaged per animal. Hemoglobin (Hb) content was directly assayed in cortical tissue after perfusion to minimize brain vascular blood using QuantiChromTM (BioAssay Systems, Hayward, CA) (He et al. 2009). Cortex tissue was weighed, homogenized in 0.1 M PBS and centrifuged 30 min/13,000 g. As per manufacture's instruction, 200 µL of reagent was mixed with 50 µL of supernatant and incubated 15 min/RT for optical density at 400 nm. Hb level was calculated as µg/g wet tissue. Perfusion decreased brain Hb by 75%–90% (Supplementary 1).

2.4. Aβ peptide immunohistochemistry

Sagittal sections (0.5–2 mm from midline at 400 um intervals), were immunostained by primary antibody Aβ (Amyloid Rabbit anti-Human, Polyclonal, Invitrogen, CA) with avidin: biotinylated immunoperoxidase (ABC Elite) and diaminobenzidine kits (Vector Laboratories, CA), (Cacciottolo et al. 2016)). For plaque quantification, 10× images were converted to 8-bit grayscale and thresholded to diminish background. Plaques were outlined for quantification by NIH ImageJ software "analyze particles" function and evaluated for percentage of area covered (Aβ load). Additionally, sections were stained for Aβ (Amyloid Rabbit anti-Human, Polyclonal, Invitrogen) and neuronal marker NeuN (mouse, Abcam, Cambridge, MA) with fluorescent secondary antibody AlexaFluor (488, goat; 594, mouse) to identify Aβ forms: a. intracellular Aβ (puncta surrounding NeuN staining; Fig. 3A, top panel) and b. extracellular Aβ plaques (globular, round, hyperintense; Fig. 3A, bottom panel). Aβ forms are shown as % of total. For CAA, Aβ-immunoreactive vessels were identified morphologically (Cacciottolo et al. 2016). Vessels were outlined to generate a CAA ROI; the CAA load was calculated as the number of immunoreactive pixels, expressed as % the total pixels.

2.5. Colocalization MBs-Aβ

After Aβ immunostaining, sections were stained by Prussian blue for hemosiderin and analyzed at 20× for co-localization with Aβ plaques (Fig. 3).

2.6. Microglia immunohistochemistry

Sagittal images were immunostained for the microglial marker Iba1 (ionized calcium-binding adapter molecule 1 (FUJIFILM Wako Chemicals, Richmond, VA). Sections were pretreated with citrate buffer (10 mM sodium citrate, 0.05% Tween, pH 6) for 5 minutes at 85 °C, followed by primary and secondary antibody with a standard avidin protocol. Iba1 images at 20X were converted to 8-bit grayscale, thresholded to diminish background, and analyzed by NIH ImageJ software. Microglia load was calculated as percentage of area covered by Iba1 immunopositive staining (Iba load).

2.7. Sholl analysis of microglial colocalization with MBs

Images were stained for Iba1 and Prussian blue (MBs) at 20× and analyzed for co-localization by FIJI (ImageJ) (Schindelin et al. 2012), followed by Sholl analysis (// Recording Sholl Analysis version 3.4.5 // Visit http://fiji.sc/Sholl#Batch_Processing for scripting examples). Intersections were recorded each 5 µm (Fig. 5C). The macroscript is available upon request.

2.8. Blood pressure

The Kent Coda Tail-Cuff system (Kent Scientific Corporation, Torrington, CT) was used to measure systolic and diastolic pressure in longitudinal (Fig.5 A-F) and cross-sectional (Supplementary Fig. 3) studies. Data of 3 consecutive days was averaged.

2.9. Fear conditioning

This test assesses the association between an aversive stimulus (mild foot shock) and a salient environmental cue of a tone or context of the test chamber, with freezing behavior as an index of fear memory. On Day 1 (acclimation/training day), mice were acclimated in the test chamber for 3 minutes and given a 20 seconds tone (75 dB), followed immediately by shock (0.3 mA). Tone-shock pairing is repeated for 5 times at 3 minutes intervals. On Day 2 ("clued day"), mice are placed in a new chamber with different walls, floor, and odor for 3 minutes. Exposure to three 20 secconds "tone-no shock" paired with a 3 minutes rest evaluates memory of tone association. Freezing time (seconds of inactivity) assesses

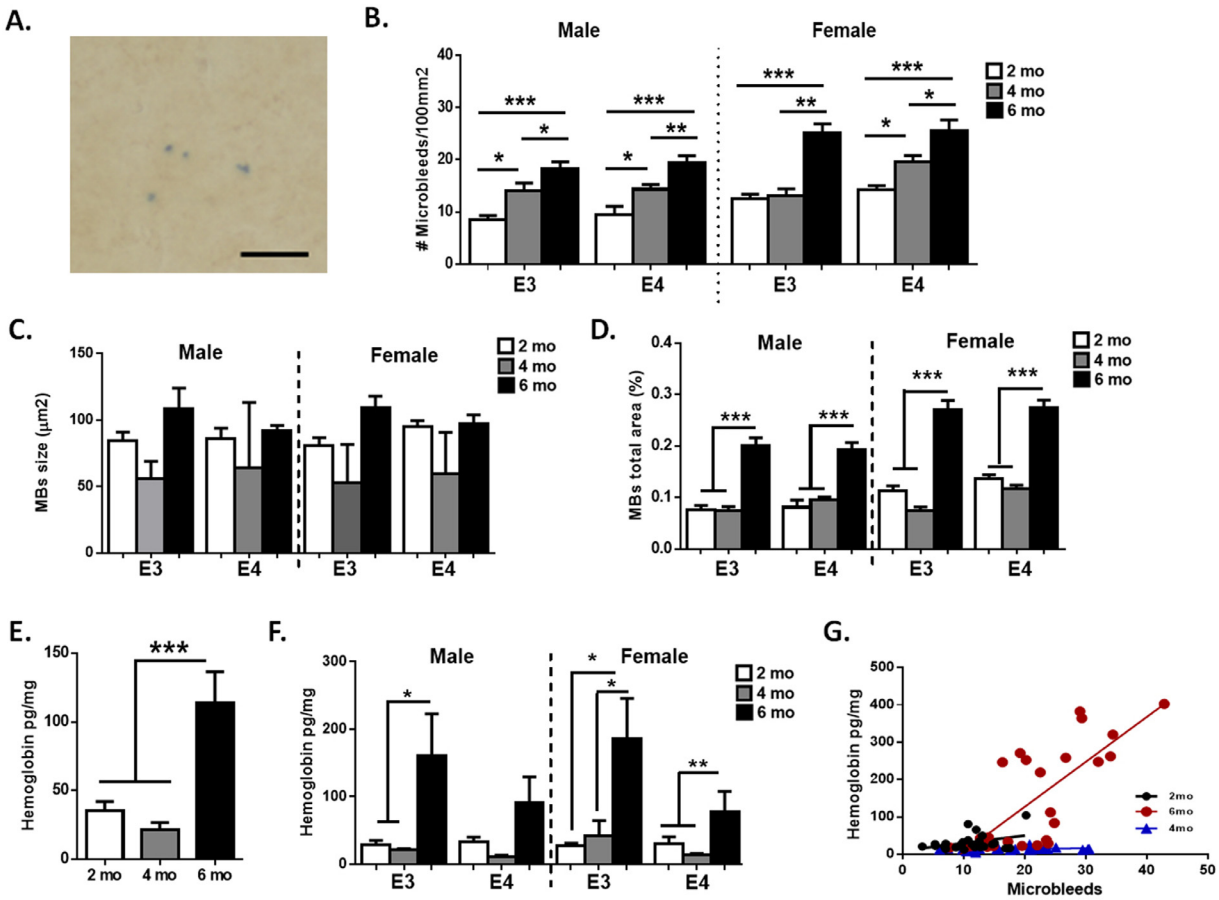

Fig. 1. Age and APOE allele effect on microbleeds (MBs). **(A)** MBs were assayed by Prussian blue histochemistry for hemosiderin (sagittal sections, 0.5–2 mm lateral from midline; scale bar: 25 µm). **(B)** Numbers of MBs increased progressively with age in both sexes and APOE alleles. (**C**) The average size of individual microbleeds did not change 2–6 months, except for the slight increase in APOE3 females. (**D**) The fractional area per section of MBs (% total area) differed by age and sex ($p < 0.001$). (**E-F**) Hemoglobin (Hb) chemically assayed. Mice aged 6 months had 2-fold more Hb than 2 and 4 months ($p < 0.01$) (all genotypes). (**F**) Hb levels correlated with MB numbers. Mean ± SEM, 6–8 mice per group. $^{*}p < 0.05$, $^{**}p < 0.01$, $^{***}p < 0.001$.

memory. On Day 3 ("context day"), mice are replaced in the same chamber as Day1 for 8 minutes, but without tone or shock. Longer freezing indicates better memory. Videos were analyzed by EthoVisionXT14 software (Noldus, Leesburg, VA). Analyses were observer blinded.

2.10. Statistics

Significance was evaluated by two-tailed t-test and two-way ANOVA with post-hoc analysis at $p < 0.05$ (GraphPad Software, San Diego, CA). Pearson correlations were run for endpoints; graphs were constructed in R studio.

3. Results

Cerebral cortex of EFAD mice was examined at 2, 4, and 6 months to define the sequence of MB and CAA accumulation in relation to amyloid deposits and microglial interactions.

3.1. MBs

MBs were present by 2 months and increased progressively with age (Fig. 1B). All genotypes had 50% more MBs and 2-fold more hemoglobin (Hb) at 6 months than 2 months. Females had 30%–50% more MBs than males at 6 months confirming (Cacciottolo et al. 2016). Also as expected, E4FAD females had ~25% more MBs than the E3FAD female ($p < 0.005$) and E4FAD male ($p < 0.01$) (Fig. 1B). The size of individual MBs was stable except for E3FAD mice, which had 15% larger deposits at age 6 months (Fig. 1C). The greater increase of MB number than size suggests that most MBs arise as a single event of extravasation, without further growth. The total area of MBs on cortex sections (hemosiderin load) increased 2-fold by 6 months ($p < 0.01$) (Fig. 1D) and with female excess.

Direct assay of Hb confirmed these age trends, with ≥ 2-fold increase for both sexes and APOE alleles by 6 months ($p < 0.001$, Fig. 1 E, F). Earlier ages did not differ for Hb by sex or APOE allele. At 6 months, E3FAD had more Hb than E4FAD, with no sex effect (Fig. 1F). At age 6 months, MBs and Hb levels were strongly correlated ($r^2 = 0.57$, $p < 0.001$, Fig. 1G), and when stratified by sex and APOE (Supplementary 2).

3.2.1. Amyloid

Two hypotheses for the development of MBs are considered (Introduction): MBs may arise by leakage from the amyloid containing cerebral blood vessels (CAA). Alternatively, MBs may arise from encroachment of extracellular Aβ amyloid plaque on cerebral vessels. These hypotheses were addressed by examining the time course and localization of MBs in relation to CAA and plaque in cortical layers by sex and APOE.

Aβ plaque load increased progressively at 2, 4, and 6 months, with greater increase in E4FAD mice (E4>E3) (Fig. 2A and B). Females had more plaques, confirming findings with 6 months old EFAD mice (Cacciottolo et al. 2016). For CAA, few vessels were

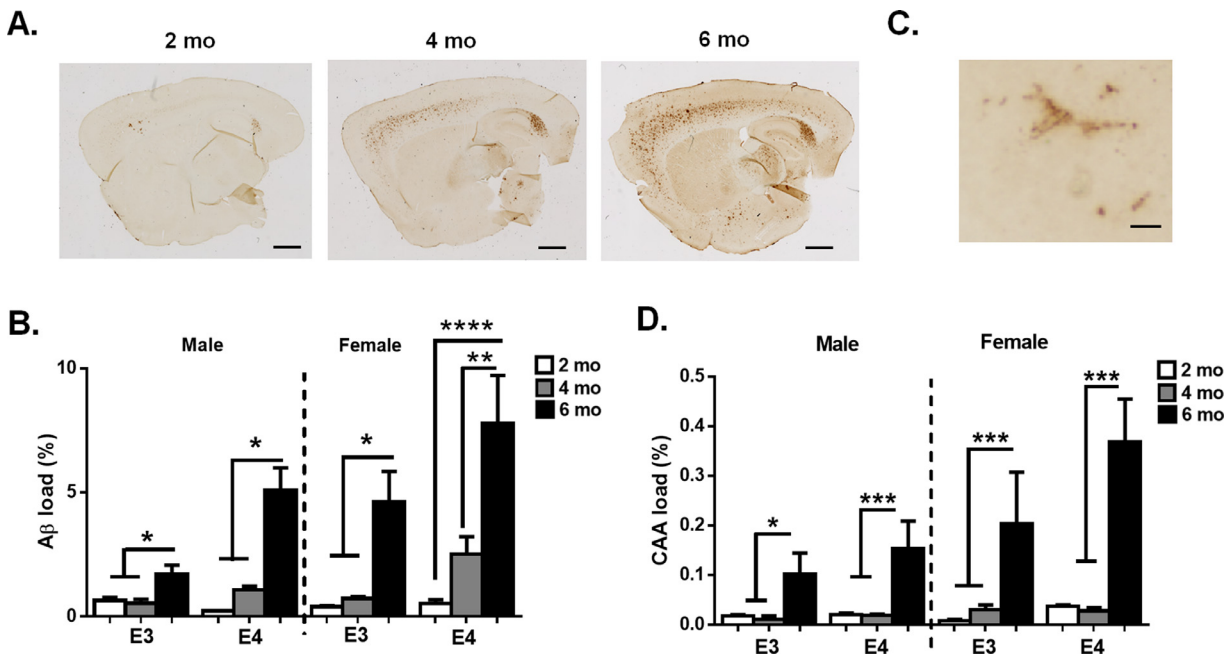

Fig. 2. Age and APOE allele effect on amyloid Aβ load. **(A)** Sagittal sections immunostained for Aβ (scale bar 1 mm). (**B**) Amyloid load as % area covered by plaques. The Aβ load increased with age in both sexes and APOE alleles of EFAD mice, 6 sections per mouse. (**C**) Amyloid stained CAA artery (Scale bar 10 µm). (**D**) CAA load. Mean ± SEM, 5–6 mice per group. $^{*}p < 0.05$, $^{**}p < 0.01$, $^{****}p < 0.001$.

Aβ positive at 2 and 4 months, followed by major increase at 6 months (>10-fold) (Fig. 2D).

At 6 mo, Aβ and CAA load were strongly correlated in all groups. Correlations were significant for both APOE alleles (E3; $r^2 = 0.5523$, $p = 0.008$; E4: $r^2 = 0.7757$, $p = 0.0088$) only in females (M: $r^2 = 0.1953$, $p = 0.1736$; F: $r^2 = 0.8026$, $p = 0.0005$). For sex and genotype, Aβ and CAA load correlation was significant only for E4FAD females (E3M: $r^2 = 0.66$, $p = 0.05$; E3F: $r^2 = 0.77$; E4M: $r^2 = 0.39$, $p = 0.26$; E4F: $r^2 = 0.83$, $p = 0.0314$).

3.2.2. Aβ accumulation: intracellular vs extracellular plaques

Cerebral cortex was stained for amyloid peptides (Aβ, green) and neurons (NeuN, red) (Fig. 3A). The Aβ staining resolved extracellular Aβ (globular) from intracellular Aβ (puncta around NeuN), shown on the enlarged images to the right (Fig. 3A, Aβ forms). The cell distribution shifted with increasing age (Fig. 3B). At 2 months, Aβ was mostly intraneuronal; at 4 months, globular extracellular Aβ appeared, and predominated at 6 months. Sex and APOE alleles modify both the intraneuronal Aβ (Fig. 3C) and Aβ plaques at 4 and 6 months, with virtually no significant effect at 2 months (Fig. 3D). Male E3FAD had consistently less plaque load at 4 and 6 months than other genotypes (Fig. 3D).

3.2.3. Colocalization of microbleeds and Aβ plaques

In prior studies, one-third of MBs in 6 months old EFAD mice were not associated with Aβ plaque ("naked MBs") (Cacciottolo et al. 2016). At age 2 months, 85% of MBs were "naked" and not contiguous with Aβ plaques in all genotypes (Fig. 4A, B). With increasing age, naked MBs became relatively less frequent as plaque amyloid numbers increased more than MBs and with co-localization (Table 1). By 6 months, 3-fold more MBs localized to Aβ plaques (Fig. 4B) than at 2 and 4 months. At 6 months, the majority of MBs and Aβ plaques were co-localized ($r^2 = 0.78$, $p < 0.0001$), confirming Cacciottolo et al. (2016). Both sex and APOE4 allele influenced the amount of MBs associated with Aβ. Females had greater association of MBs with Aβ at 6 mo than younger ages

Table 1
Ratio MBs:Aβ plaques

MB:Aβ plaques	E3M	E3F	E4M	E4F
2mo	2.5:1	2:1	1.4:1	1.6:1
4mo	1.2:1	0.2:1	0.3:1	0.3:1
6mo	0.2:1	0.1:1	0.1:1	0.1:1

for E3FAD (3-fold, $p < 0.01$) and E4FAD (2-fold, $p < 0.01$). Moreover, 6 months male E4FAD had 2-fold ($p < 0.05$) more MBs associated with Aβ than E3FAD and younger ages. The changing ratios of MB:Aβ plaque suggests that MBs, which precede Aβ plaques, may seed their formation.

3.4.1. Localization of MBs, Aβ plaque load, and CAA in cortical layers

The localization of MBs, Aβ plaque load and CAA was further analyzed by cerebral cortex layer (Fig. 5A). Most MBs (90%) occurred in deeper layers (3-5), where smaller arteries are prevalent. Outer layers (1-2) containing larger vessels had ~10% of all MBs (Fig. 5B and C). MBs arose in all cortical layers, with no evident age difference (Fig. 5B and C). At 2 months, the Aβ plaque load was greatest in cortical layer 4 (Fig. 4A, B, E), followed by its spread into layer 5 at 4 months. By 6 months, most plaques occurred in layers 4, 5, and 6 (Fig. 5E).

CAA had a different localization than MBs and plaques (Fig. 5B-D). At 2 months, CAA was restricted to outer cortical layers (1–3) (Fig. 5D). At 4 and 6 months, CAA increased in deeper layers (4–6), in parallel with the accumulating Aβ plaques and load (Fig. 5D).

3.4.2. Microglial distribution in relation to MBs

Iba1-immunostaine microglia increased after 2 mo (Fig. 6A, B) and remained the same at 4 and 6 months (Male: E3 +45%, $p < 0.05$; E4 +20%, ns; Female: E3 +80%, $p < 0.05$; E4 +40%, $p < 0.05$). Microglial activation was evaluated as the colocalization of MBs with microglial processes by Sholl analysis (Fig. 6C and D). The number of intersections with microglial processes increased with distance from the center of individual microbleeds (10 µm distance

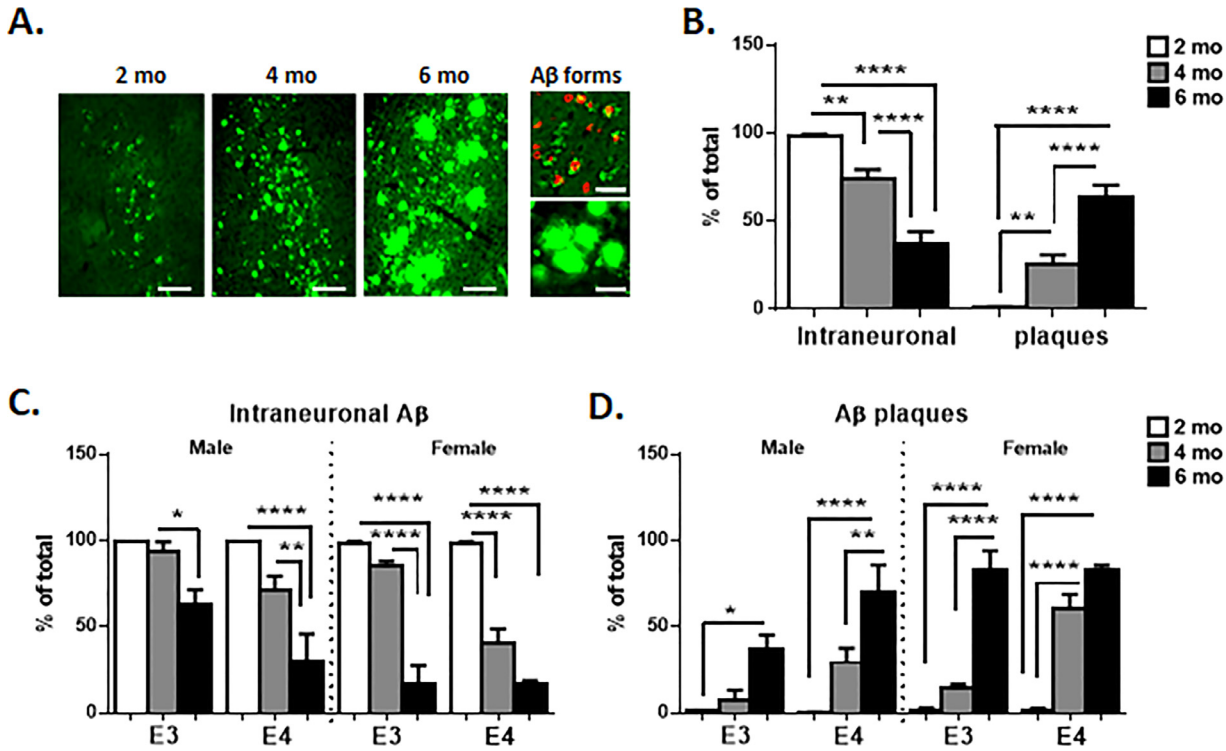

Fig. 3. Intraneuronal Aβ and Aβ plaques. **(A)** Aβ immunostaining by age (size bar: 100 µm). Aβ forms are illustrated in Aβ forms (right panels): top panel, intraneuronal Aβ (green) colocalized with NeuN (red; size bar: 25 µm); lower panel, extracellular Aβ plaques (size bar: 100 µm). **(B)** Age decrease in relative amount of intraneuronal Aβ and increase of extracellular Aβ plaques. **(C)** Intraneuronal Aβ stratified by age, sex and APOE allele. **(D)** Aβ plaques stratified by age, sex and APOE allele. See Supplementary Table 1 for % and absolute numbers of intraneuronal Aβ and Aβ plaques. Mean ± SEM, 5–6 mice per group. $^{*}p < 0.05$, $^{**}p < 0.01$, $^{****}p < 0.001$. (For interpretation of the references to color in this figure legend, the reader is referred to the Web version of this article.)

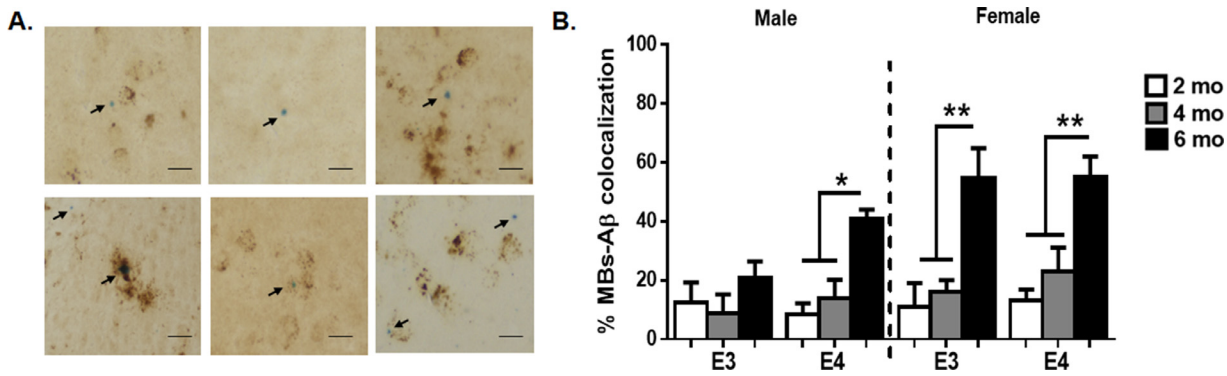

Fig. 4. Co-localization of MBs and Aβ plaques in cerebral cortex. **(A)** Co-staining of MBs (Prussian blue histochemistry) and Aβ plaques. Arrows point to MBs. Top row images show minimal colocalization; bottom row images show extensive colocalization. **(B)** Co-localization data. Mean ± SEM, 5–6 mice per group. Scale bar: 10 µm. $^{*}p < 0.05$, $^{**}p < 0.01$. (For interpretation of the references to color in this figure legend, the reader is referred to the Web version of this article.)

had 50% more than 5 µm. This trend is opposite than expected for a role of MB in microglial activation and did not differ by sex or APOE allele.

3.5. Blood pressure in EFAD mice

Because hypertension is associated with MBs in human and because C57BL/6 female mice show trends for elevated blood pressure at 6 months (Intro), we evaluated blood pressure from age 2 to 6 months. Tail cuffing, a minimally invasive procedure, gave the same finding with longitudinal (Fig. 7) and cross-sectional studies (Suppl.3). Systolic and diastolic pressures did not differ by sex or APOE at 2 mo (Fig. 7A, D) and 4 months (Fig. 7B and C). However, at 6 months female E3FAD mice had higher systolic pressure than males (+15%, $p < 0.05$, Fig. 7C, F). the E4FAD females showed a non-significant trend. These findings discount a role for increased blood pressure for the large increase of MBs in young adult EFAD mice.

3.6. Evaluation of memory by fear conditioning

The fear conditioning test evaluated relationships of cognition to MBs and amyloid. Freezing time was assessed on day 2 (cued fear conditioning) and on day 3 (context fear conditioning). On day 2 (cued fear conditioning), 2 months old E4FAD mice freeze less compared to E3FAD mice. Similar behavior is observed in both

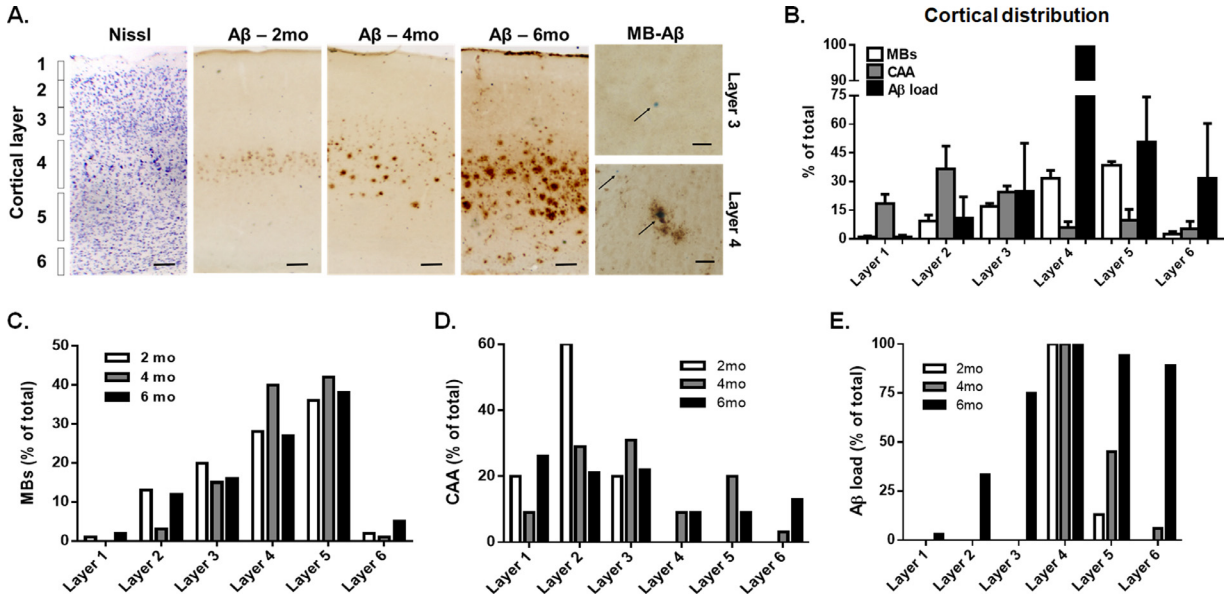

Fig. 5. MBs, Aβ plaques, and CAA by cerebral cortex layers. **(A)** Staining for Aβ and Nissl with identification of cortical layer (scale bar 100 µm), and MBs (arrows, scale bar 10 µm). **(B)** Layer distribution of MBs, Aβ plaques and CAA, shown as % of total for each age group. **(C)** MBs mainly occurred in deeper cortical layers (4–5) with minor differences in layer-wise distribution by age. **(D)** CAA in cortical layer by ages. CAA localization differed by ages, detected in outer layers (1–3) at 2 months, and expanding with age to inner layers at 4 and 6 months. **(E)** Aβ plaques (load) by cortical layer. At 2 months, Aβ plaques occurred mainly in layer 4 and expanded to the inner layers with age. Means ± SEM, 5–6 mice per group.

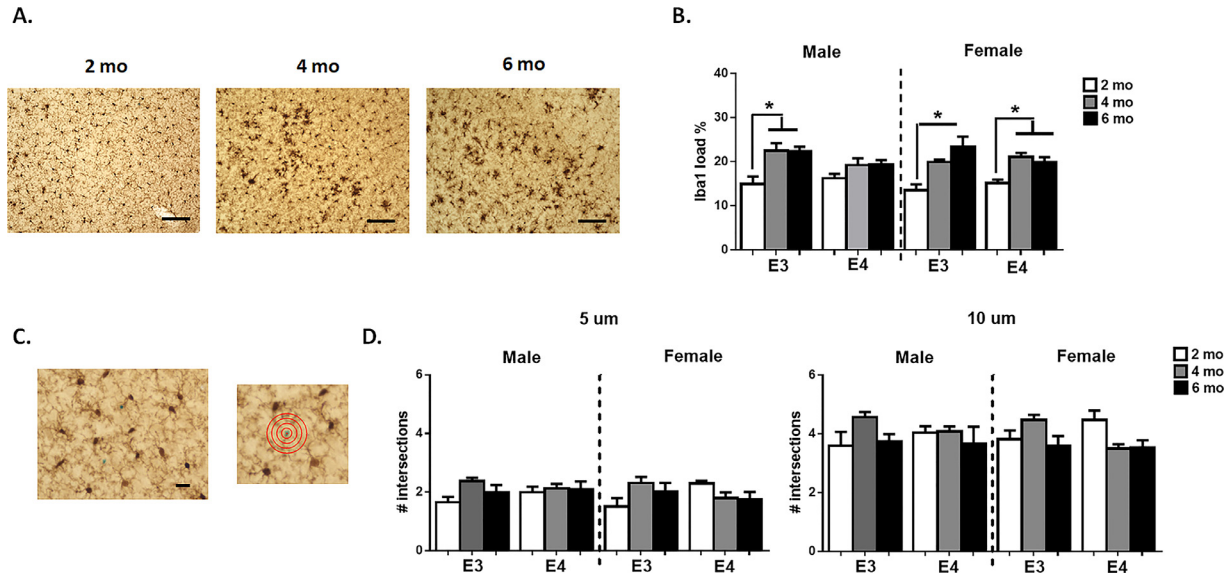

Fig. 6. Age and microglia. **(A)** Iba1 immunostained microglia in cerebral cortex (Scale bar 100 µ). **(B)** Iba1 load by age, sex, and APOE. **(C)** Co-staining for microglia (IBA1) and MBs (Prussian blue) (Scale bar 20 µm). The smaller square shows concentric circles spaced at 5 µm, with center on a MB for Sholl analysis. **(D)** Numbers of microglial processes within 5 and 10 µm of MB. Mean ± SEM, 5–6 mice per group. $^{*}p < 0.05$, $^{**}p < 0.01$. (For interpretation of the references to color in this figure legend, the reader is referred to the Web version of this article.)

male (E4<E3, −50%, $p < 0.05$) and female (E4<E3, −33%, not significant) (Fig. 8). While E3FAD did not differ by sex, E4FAD female mice had a slightly greater freezing time (M<F, −25%, not significant). At 4 months, EFAD mice did not differ from 2 months old. Freezing time of E3FAD both sexes decreased by 50% after 4 months. Freezing time decreased in E4FAD male (E4<E3, −50%, $p < 0.05$) and female (E4<E3, −50%, $p < 0.05$). At 6 months, the groups did not differ by sex or APOE. Notably, the freezing time at age 6 months was identical to younger E4FAD mice (~150s total freezing time). On day 3, no differences were observed across experimental groups by age, sex or APOE allele (not shown).

3.7. Correlations and interactions

Interactions were evaluated by Pearson correlation analysis (Fig. 9, Table 1). Positive correlations were found for MBs, Aβ load and CAA (Table 2). Blood pressure did not correlate with any of the endpoints of MBs, Aβ or inflammation. Fear conditioning on the cue day was negatively correlated with MBs ($r^2 = -0.97$, $p = 0.005$), Aβ load ($r^2 = -0.96$, $p = 0.007$), and CAA ($r^2 = -0.93$, $p = 0.02$). Iba1 and fear conditioning showed weak inverse correlation ($r^2 = -0.84$, $p = 0.07$), but did not correlate with MBs or amyloid plaque or CAA.

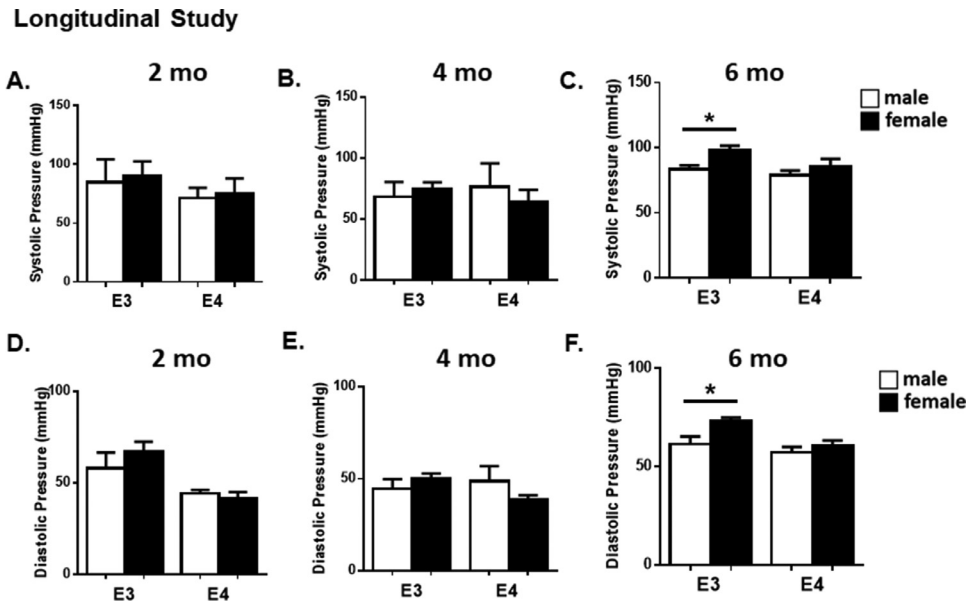

Fig. 7. Blood pressure, longitudinal study. **(A-C)** systolic and **(D-F)** diastolic blood pressure. Female E3FAD mice at 6 months had higher systolic and diastolic pressures than male mice. Repeated measurements over 3 days were averaged. Concurrent cross-sectional studies gave identical results of stable blood pressure, again with the exception of elevations in female E3FAD (Supplementary 3). Mean ± SEM, 5–6 mice per group. * $p < 0.05$.

Table 2
Matrix of correlations

MB#	Aβ load	CAA	Iba1	FC-cue	
1	$r^2 = 0.97$ $p = 0.004$	$r^2 = 0.94$ $p = 0.02$	$r^2 = 0.75$ $p = 0.14$	r2 = −0.97 $p = 0.005$	**MB#**
		$r^2 = 0.98$ $p = 0.003$	$r^2 = 0.68$ $p = 0.2$	$r^2 = -0.96$ $p = 0.007$	**Aβ load**
		1	$r^2 = 0.60$ $p = 0.28$	$r^2 = -0.93$ $p = 0.02$	**CAA**
			1	$r^2 = -0.84$ $p = 0.07$	**Iba1**
				1	**FC-cue**

4. Discussion

This study examined temporal relationships between MBs, extracellular amyloid and CAA in the EFAD mouse cerebral cortex. At age 2 months, most (85%) of MBs were “naked” and did not contact the few extracellular amyloid plaques. The subsequent increase of plaque numbers was greater than the increased numbers of MBs, with a lower ratio of MBs:Aβ plaques by age 6 months. The relative stability of plaque size during major increase of total amyloid in EFAD mice parallels human AD, in which plaque area remained constant during disease duration of more than ten years (Haller et al. 2019).

The greater increase of MB number without increased size in EFAD mice suggests that most MBs arise as a single event, and do not grow from further extravasation. These findings support the hypothesis that extracellular amyloid plaques are seeded by MBs (Cullen et al. 2006; Cacciottolo et al. 2016). Other supporting evidence is the rapid formation of amyloid deposits around needle tracks in wildtype mouse (Chuang et al. 2012) and rat (Purushothuman et al. 2013), and the rapid increase of fibrillary amyloid in the APP/PS1 AD mouse after laser induced ischemia (Zhang et al. 2019).

MBs and CAA increased in different cortical layers: while CAA was most prevalent in outer layers, most plaques and MBs arose in deeper layers 4 and 5. The spatial disparity of extracellular amyloid and CAA was also shown in postmortem human brain (van Veluw et al. 2017; van Veluw et al. 2020). Together, these findings weaken the hypothesis that MBs arise from the damaged vasculature of CAA in agreement with (van Veluw et al. 2019; van Veluw et al. 2020).

We also evaluated the potential role of blood pressure during ages 2, 4, and 6 months in EFAD mice because hypertension increases MB risk in humans (Intro). Systolic and diastolic blood pressure did not differ by age, sex, or APOE4 except for E3FAD females which showed a small increase of blood pressure at age 6 months that was within the normative range. These observations generally agree with a Framingham study of 472 subjects which associated MBs with advanced age and sex, but not with blood pressure (Jeerakathil et al. 2004).

Pearson correlations further documented these findings. All endpoints except blood pressure were correlated to some degree to the MBs. The inverse correlation of memory score and MBs aligns with the Framingham Heart Study (FHS), in which the risk of dementia was increased 1.7-fold in those with MBs (Romero et al. 2017). Interactions of amyloid and MB on cognitive deficits cannot be resolved in the present study.

The blood-brain barrier (BBB) and neurovascular unit need evaluation for roles in MBs. The 5xFAD mouse developed microvascular leakage by age 4 months (Giannoni et al. 2016). While the leakage was concurrent with Aβ plaques, neuronal Aβ traces of Aβ were present at 2 months. The microcapillary leakage was not considered significant until 9 mo. Perivascular pericytes increased progressively after 4 months.

In mouse and human studies, the CSF levels of PDGFRβ (pericyte injury) were correlated with increased activity of the BBB-degrading cyclophilin A-matrix metalloproteinase-9 pathway in APOE4 carriers (Bell et al. 2012; Montagne et al. 2020). Vascular endothelial changes in EFAD mice were shown by response of 8 months old E4FAD female mice to 2 mo treatment with epidermal growth factor (EGF), which improved BBB integrity, while not alter-

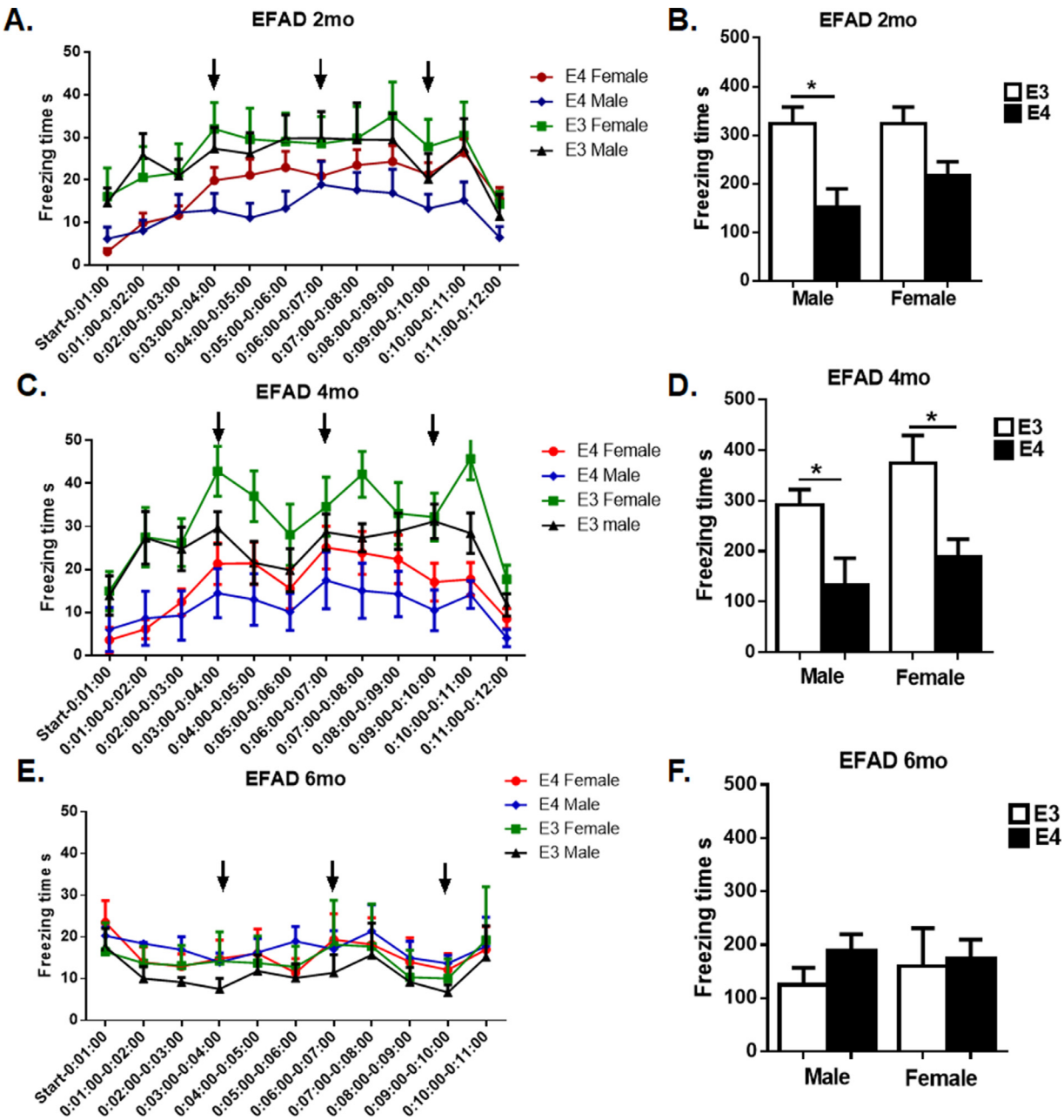

Fig. 8. Fear conditioning of memory. Memory ability was recorded as freezing time on day 2. Freezing time is graphed as seconds of inactivity (freezing) per time interval (A, C, E) and total freezing time (B, D, F). (**A-B**) At 2 months, APOE4 had shorter freezes than APOE3, in both sexes (E4<E3, −50%, $p < 0.05$). (**D**) Ages 2 and 4 months had similar decrease of freezing time in both sexes: male (E4<E3, −50%, $p < 0.05$) and female (E4<E3, −50%, $p < 0.05$). (**E-F**) At 6 months, groups did not differ by sex or APOE; freezing time was similar to younger E4FAD (~150 seconds total freezing). Mean ± SEM, 8–10 mice/group. * $p < 0.05$.

ing Aβ levels. The EGF treatment greatly decreased the number of existing MBs (Thomas et al. 2016), implying further mechanisms of clearance with systemic physiological interaction. Astrocytes may contribute to MBs through extravasation because of their close interactions with pericytes (Sweeney et al. 2019). Tau also merits evaluation in EFAD mice for relation to MBs because tau was co-localized with needle track amyloid (Purushothuman et al. 2013), while blood tau was associated with MB incidence in the FHS (Romero et al. 2020). The levels of oxidative damage in AD brains for APOE alleles parallels their AD risk: APOE4>E3>E2. (Butterfield and Mattson, 2020)

Lastly, we note that other forms of cerebral extravasation increase in parallel with cerebral MBs during human aging. In advanced cases of human CAA, van Veluw et al. (2019) distinguished cerebral MBs from cerebral microinfarcts, which were associated fibrillar amyloid, unlike the MBs in that sample, suggesting that CAA fosters multiple pathophysiological mechanisms (van Veluw et al. 2019). The diversity and complexity of cerebrovascular pathologies is increasingly recognized in forms of brain arteriolosclerosis that lack atheromas and vascular amyloid (Blevins et al. 2020).

5. Limitations of this study

The numbers of mice per group were limited to 5–6 mice per group because of the workload in comparing four EFAD geno-

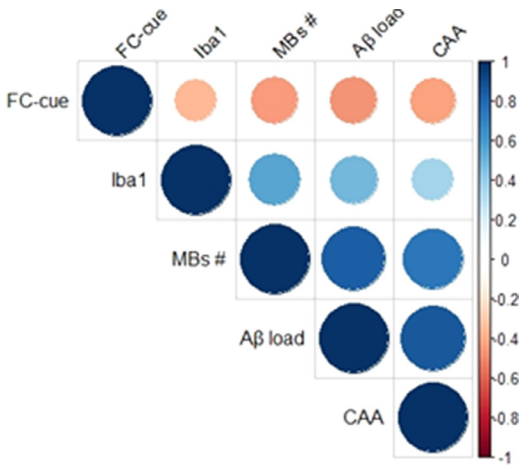

Fig. 9. Correlations. Pearson correlations were analyzed for possible interactions. Abbreviations: FC, fear conditioning; MBs, microbleeds; MBs # microbleed number; CAA, cerebrovascular amyloid angiopathy.

types (both sexes, 2 ApoE alleles). Nonetheless, findings for age 6 months confirm our initial study of EFAD mice at age 6 months (Cacciottolo et al. 2016). Future studies might consider use of sibling non-carrier FAD mice, where the absence of human Aβ might reveal additional APOE allele effects.

6. Conclusions

Prior studies associated MBs with amyloid deposits, suggesting a causal relationship, which is further supported by these studies of the time course of pathology in cerebral cortex layers of young EFAD mice. MBs originate in deep cortical layers in direct contact with extracellular amyloid plaques at age 2 months, whereas CAA is most prevalent in outer layer 4. The earlier emergence of MBs contiguous with plaques support the hypothesis that MBs seed amyloid deposition. Their early occurrence and location discount CAA as a major contributor to MBs. Memory, assessed by fear conditioning, decreased by 6 mo in correlation with MBs and amyloid. Female E4FAD mice had the most pathology.

Author contribution

Mafalda Cacciottolo: conceptualization, methodology, data acquisition, data analysis, writing; **Todd E. Morgan:** conceptualization, funding acquisition, writing; **Caleb E. Finch:** conceptualization, funding acquisition, writing.

Disclosure statement

The authors have no conflicts of interest to disclose.

Acknowledgements

We are grateful for support by Cure Alzheimer's Fund and National Institute on Aging R21 AG050201, R01 AG051521, P01 AG055367 and P50 AG005142. We appreciate critical reading by Christian Pike (USC) and Axel Montaigne (University of Edinburgh).

Supplementary materials

Supplementary material associated with this article can be found, in the online version, at doi:10.1016/j.neurobiolaging.2021.02.020.

References

Akoudad, S., Wolters, F.J., Viswanathan, A., de Bruijn, R.F., van der Lugt, A., Hofman, A., Koudstaal, P.J., Ikram, M.A., Vernooij, M.W., 2016. Association of cerebral microbleeds with cognitive decline and dementia. JAMA Neurol 73 (8), 934–943. doi:10.1001/jamaneurol.2016.1017.

Bell, R.D., Winkler, E.A., Singh, I., Sagare, A.P., Deane, R., Wu, Z., Holtzman, D.M., Betsholtz, C., Armulik, A., Sallstrom, J., Berk, B.C., Zlokovic, B.V., 2012. Apolipoprotein E controls cerebrovascular integrity via cyclophilin A. Nature 485 (7399), 512–516. doi:10.1038/nature11087.

Biffi, A., Murphy, M.P., Kubiszewski, P., Kourkoulis, C., Schwab, K., Gurol, M.E., Greenberg, S.M., Viswanathan, A., Anderson, C.D., Rosand, J., 2019. APOE genotype, hypertension severity and outcomes after intracerebral haemorrhage. Brain Commun. 1 (1), fcz018. doi:10.1093/braincomms/fcz018.

Blevins, B.L., Vinters, H.V., Love, S., Wilcock, D.M., Grinberg, L.T., Schneider, J.A., Kalaria, R.N., Katsumata, Y., Gold, B.T., Wang, D.J.J., Ma, S.J., Shade, L.M.P., Fardo, D.W., Hartz, A.M.S., Jicha, G.A., Nelson, K.B., Magaki, S.D., Schmitt, F.A., Teylan, M.A., Ighodaro, E.T., Phe, P., Abner, E.L., Cykowski, M.D., Van Eldik, L.J., Nelson, P.T, 2020. Brain arteriolosclerosis. Acta Neuropathol. doi:10.1007/s00401-020-02235-6.

Butterfield, D.A., Mattson, M.P., 2020. Apolipoprotein E and oxidative stress in brain with relevance to Alzheimer's disease. Neurobiol. Dis. 138, 104795. doi:10.1016/j.nbd.2020.104795.

Cacciottolo, M., Christensen, A., Moser, A., Liu, J., Pike, C.J., Smith, C., LaDu, M.J., Sullivan, P.M., Morgan, T.E., Dolzhenko, E., Charidimou, A., Wahlund, L.O., Wiberg, M.K., Shams, S., Chiang, G.C., Finch, C.E.Alzheimer's Disease Neuroimaging, I, 2016. The APOE4 allele shows opposite sex bias in microbleeds and Alzheimer's disease of humans and mice. Neurobiol. Aging 37, 47–57. doi:10.1016/j.neurobiolaging.2015.10.010.

Charidimou, A., Shams, S., Romero, J.R., Ding, J., Veltkamp, R., Horstmann, S., Eiriksdottir, G., van Buchem, M.A., Gudnason, V., Himali, J.J., Gurol, M.E., Viswanathan, A., Imaizumi, T., Vernooij, M.W., Seshadri, S., Greenberg, S.M., Benavente, O.R., Launer, L.J., Shoamanesh, A., International, M.-M.I., 2018. Clinical significance of cerebral microbleeds on MRI: A comprehensive meta-analysis of risk of intracerebral hemorrhage, ischemic stroke, mortality, and dementia in cohort studies (v1). Int. J. Stroke 13 (5), 454–468. doi:10.1177/1747493017751931.

Chuang, J.Y., Lee, C.W., Shih, Y.H., Yang, T., Yu, L., Kuo, Y.M., 2012. Interactions between amyloid-beta and hemoglobin: implications for amyloid plaque formation in Alzheimer's disease. PLoS One 7 (3), e33120. doi:10.1371/journal.pone.0033120.

Cullen, K.M., Kocsi, Z., Stone, J., 2006. Microvascular pathology in the aging human brain: evidence that senile plaques are sites of microhaemorrhages. Neurobiol. Aging 27 (12), 1786–1796. doi:10.1016/j.neurobiolaging.2005.10.016.

Diaz-Otero, J.M., Garver, H., Fink, G.D., Jackson, W.F., Dorrance, A.M., 2016. Aging is associated with changes to the biomechanical properties of the posterior cerebral artery and parenchymal arterioles. Am J Physiol Heart Circ Physiol 310 (3), H365–H375. doi:10.1152/ajpheart.00562.2015.

Fisher, M., 2014. Cerebral microbleeds: where are we now? Neurology 83 (15), 1304–1305. doi:10.1212/WNL.0000000000000871.

Fisher, M., French, S., Ji, P., Kim, R.C., 2010. Cerebral microbleeds in the elderly: a pathological analysis. Stroke 41 (12), 2782–2785. doi:10.1161/STROKEAHA.110.593657.

Gong, L., Tian, X., Zhou, J., Dong, Q., Tan, Y., Lu, Y., Wu, J., Zhao, Y., Liu, X., 2019. Iron dyshomeostasis induces binding of APP to BACE1 for amyloid pathology, and impairs APP/Fpn1 complex in microglia: implication in pathogenesis of cerebral microbleeds. Cell Transplant 28 (8), 1009–1017. doi:10.1177/0963689719831707.

Giannoni, P, Arango-Lievano, M, Neves, ID, Rousset, MC, Baranger, K, Rivera, S, Jeanneteau, F, Claeysen, S, Marchi, N., 2016. Cerebrovascular pathology during the progression of experimental Alzheimer's disease. Neurobiol Dis 88, 107–117. doi:10.1016/j.nbd.2016.01.001.

Graff-Radford, J., Lesnick, T., Rabinstein, A.A., Gunter, J., Aakre, J., Przybelski, S.A., Spychalla, A.J., Huston 3rd, J., Brown Jr., R.D., Mielke, M.M., Lowe, V.J., Knopman, D.S., Petersen, R.C., Jack Jr, C.R., Vemuri, P., Kremers, W., Kantarci, K, 2020. Cerebral microbleed incidence, relationship to amyloid burden: the Mayo Clinic Study of Aging. Neurology 94 (2), e190–e199. doi:10.1212/WNL.0000000000008735.

Greenberg, S.M., Vernooij, M.W., Cordonnier, C., Viswanathan, A., Salman, Al-Shahi, R., Warach, S., Launer, J., L., Van Buchem, M.A., Breteler, M.M.Microbleed Study, G, 2009. Cerebral microbleeds: a guide to detection and interpretation. Lancet Neurol. 8 (2), 165–174. doi:10.1016/S1474-4422(09)70013-4.

Gregoire, S.M., Chaudhary, U.J., Brown, M.M., Yousry, T.A., Kallis, C., Jager, H.R., Werring, D.J., 2009. The Microbleed Anatomical Rating Scale (MARS): reliability of a tool to map brain microbleeds. Neurology 73 (21), 1759–1766. doi:10.1212/WNL.0b013e3181c34a7d.

Haller, S., Scheffler, M., Salomir, R., Herrmann, F.R., Gold, G., Montandon, M.L., Kovari, E., 2019. MRI detection of cerebral microbleeds: size matters. Neuroradiology 61 (10), 1209–1213. doi:10.1007/s00234-019-02267-0.

He, Y., Hua, Y., Liu, W., Hu, H., Keep, R.F., Xi, G., 2009. Effects of cerebral ischemia on neuronal hemoglobin. J Cereb Blood Flow Metab 29 (3), 596–605. doi:10.1038/jcbfm.2008.145.

Jeerakathil, T., Wolf, P.A., Beiser, A., Hald, J.K., Au, R., Kase, C.S., Massaro, J.M., DeCarli, C., 2004. Cerebral microbleeds: prevalence and associations with cardiovascular risk factors in the Framingham Study. Stroke 35 (8), 1831–1835. doi:10.1161/01.STR.0000131809.35202.1b.

Jia, Z., Mohammed, W., Qiu, Y., Hong, X., Shi, H., 2014. Hypertension increases the risk of cerebral microbleed in the territory of posterior cerebral artery: a study of the association of microbleeds categorized on a basis of vascular territories and cardiovascular risk factors. J. Stroke Cerebrovasc. Dis. 23 (1), e5–11. doi:10.1016/j.jstrokecerebrovasdis.2012.12.016.

Keller, K., Kane, A., Heinze-Milne, S., Grandy, S.A., Howlett, S.E., 2019. Chronic treatment with the ACE inhibitor enalapril attenuates the development of frailty and differentially modifies pro- and anti-inflammatory cytokines in aging male and female C57BL/6 mice. J. Gerontol. A Biol. Sci. Med. Sci. 74 (8), 1149–1157. doi:10.1093/gerona/gly219.

Knol, M.J., Lu, D., Traylor, M., Adams, H.H., Rafael, J.R.J., Smith, A.V., Fornage, M., Hofer, E., Liu, J., Hostettler, I.C., Luciano, M., Trompet, S., Giese, A.K., Hilal, S., van den Akker, E.B., Vojinovic, D., Li, S., Sigurdsson, S., van der Lee, S.J., Jack Jr., C.R., Wilson, D., Yilmaz, P., Satizabal, C.L., Liewald, D.C.M., van der Grond, J., Chen, C., Saba, Y., van der Lugt, A., Bastin, M.E., Windham, B.G., Cheng, C.Y., Pirpamer, L., Kantarci, K., Himali, J.J., Yang, Q., Morris, Z., Beiser, A.S., Tozer, D.J., Vernooij, M.W., Amin, N., Beekman, M., Koh, J.Y., Stott, D.J., Houlden, H., Schmidt, R., Gottesman, R.F., MacKinnon, A.D., DeCarli, C., Gudnason, V., Deary, I.J., van Duijn, C.M., Slagboom, P.E., Wong, T.Y., Rost, N.S., Jukema, J.W., Mosley, T.H., Werring, D.J., Schmidt, H., Wardlaw, J.M., Ikram, M.A., Seshadri, S., Launer, L.J., Markus, H.SAlzheimer's Disease Neuroimaging, I, 2020. Association of common genetic variants with brain microbleeds: a Genome-wide Association Study. Neurology doi:10.1212/WNL.0000000000010852.

Li, H.Q., Cai, W.J., Hou, X.H., Cui, M., Tan, L., Yu, J.T., Dong, Q.Alzheimer's Disease Neuroimaging, I., 2020. Genome-wide association study of cerebral microbleeds on MRI. Neurotox. Res. 37 (1), 146–155. doi:10.1007/s12640-019-00073-3.

Liu, W., Liu, R., Sun, W., Peng, Q., Zhang, W., Xu, E., Cheng, Y., Ding, M., Li, Y., Hong, Z., Wu, J., Zeng, J., Yao, C., Huang, Y., Group, C.S., 2012. Different impacts of blood pressure variability on the progression of cerebral microbleeds and white matter lesions. Stroke 43 (11), 2916–2922. doi:10.1161/STROKEAHA.112.658369.

Montagne, A., Nation, D.A., Sagare, A.P., Barisano, G., Sweeney, M.D., Chakhoyan, A., Pachicano, M., Joe, E., Nelson, A.R., D'Orazio, L.M., Buennagel, D.P., Harrington, M.G., Benzinger, T.L.S., Fagan, A.M., Ringman, J.M., Schneider, L.S., Morris, J.C., Reiman, E.M., Caselli, R.J., Chui, H.C., Tcw, J., Chen, Y., Pa, J., Conti, P.S., Law, M., Toga, A.W., Zlokovic, B.V, 2020. APOE4 leads to blood-brain barrier dysfunction predicting cognitive decline. Nature 581 (7806), 71–76. doi:10.1038/s41586-020-2247-3.

Nyul-Toth, A., Tarantini, S., Kiss, T., Toth, P., Galvan, V., Tarantini, A., Yabluchanskiy, A., Csiszar, A., Ungvari, Z., 2020. Increases in hypertension-induced cerebral microhemorrhages exacerbate gait dysfunction in a mouse model of Alzheimer's disease. Geroscience doi:10.1007/s11357-020-00256-3.

Petrea, R.E., O'Donnell, A., Beiser, A.S., Habes, M., Aparicio, H., DeCarli, C., Seshadri, S., Romero, J.R., 2020. Mid to late life hypertension trends and cerebral small vessel disease in the Framingham Heart Study. Hypertension 76 (3), 707–714. doi:10.1161/HYPERTENSIONAHA.120.15073.

Poels, M.M., Vernooij, M.W., Ikram, M.A., Hofman, A., Krestin, G.P., van der Lugt, A., Breteler, M.M., 2010. Prevalence and risk factors of cerebral microbleeds: an update of the Rotterdam scan study. Stroke 41 (10 Suppl), S103–S106. doi:10.1161/STROKEAHA.110.595181.

Purushothuman, S., Marotte, L., Stowe, S., Johnstone, D.M., Stone, J., 2013. The response of cerebral cortex to haemorrhagic damage: experimental evidence from a penetrating injury model. PLoS One 8 (3), e59740. doi:10.1371/journal.pone.0059740.

Romero, J.R., Beiser, A., Himali, J.J., Shoamanesh, A., DeCarli, C., Seshadri, S., 2017. Cerebral microbleeds and risk of incident dementia: the Framingham Heart Study. Neurobiol. Aging 54, 94–99. doi:10.1016/j.neurobiolaging.2017.02.018.

Romero, J.R., Demissie, S., Beiser, A., Himali, J.J., DeCarli, C., Levy, D., Seshadri, S., 2020. Relation of plasma beta-amyloid, clusterin, and tau with cerebral microbleeds: Framingham Heart Study. Ann. Clin. Transl. Neurol. 7 (7), 1083–1091. doi:10.1002/acn3.51066.

Schindelin, J., Arganda-Carreras, I., Frise, E., Kaynig, V., Longair, M., Pietzsch, T., Preibisch, S., Rueden, C., Saalfeld, S., Schmid, B., Tinevez, J.Y., White, D.J., Hartenstein, V., Eliceiri, K., Tomancak, P., Cardona, A., 2012. Fiji: an open-source platform for biological-image analysis. Nat. Methods 9 (7), 676–682. doi:10.1038/nmeth.2019.

Shi, J., Liu, Y., Liu, Y., Li, Y., Qiu, S., Bai, Y., Gu, Y., Luo, J., Cui, H., Li, Y., Zhao, Q., Zhang, K., Cheng, Y., 2018. Association between ApoE polymorphism and hypertension: a meta-analysis of 28 studies including 5898 cases and 7518 controls. Gene 675, 197–207. doi:10.1016/j.gene.2018.06.097.

Sullivan, P.M., Mace, B.E., Estrada, J.C., Schmechel, D.E., Alberts, M.J., 2008. Human apolipoprotein E4 targeted replacement mice show increased prevalence of intracerebral hemorrhage associated with vascular amyloid deposition. J. Stroke Cerebrovasc. Dis. 17 (5), 303–311. doi:10.1016/j.jstrokecerebrovasdis.2008.03.011.

Sweeney, M.D., Zhao, Z., Montagne, A., Nelson, A.R., Zlokovic, B.V., 2019. Blood-brain barrier: from physiology to disease and back. Physiol. Rev. 99 (1), 21–78. doi:10.1152/physrev.00050.2017.

Tanifum, E.A., Starosolski, Z.A., Fowler, S.W., Jankowsky, J.L., Annapragada, A.V., 2014. Cerebral 543 vascular leak in a mouse model of amyloid neuropathology. J Cereb Blood Flow Metab. 34 (10), 1646–1654. doi:10.1038/jcbfm.2014.125.

Thomas, R., Zuchowska, P., Morris, A.W., Marottoli, F.M., Sunny, S., Deaton, R., Gann, P.H., Tai, L.M., 2016. Epidermal growth factor prevents APOE4 and amyloid-beta-induced cognitive and cerebrovascular deficits in female mice. Acta Neuropathol. Commun. 4 (1), 111. doi:10.1186/s40478-016-0387-3.

van Veluw, S.J., Frosch, M.P., Scherlek, A.A., Lee, D., Greenberg, S.M., Bacskai, B.J., 2020. In vivo characterization of spontaneous microhemorrhage formation in mice with cerebral amyloid angiopathy. J Cereb Blood Flow Metab doi:10.1177/0271678X19899377, 271678X19899377.

van Veluw, S.J., Kuijf, H.J., Charidimou, A., Viswanathan, A., Biessels, G.J., Rozemuller, A.J., Frosch, M.P., Greenberg, S.M., 2017. Reduced vascular amyloid burden at microhemorrhage sites in cerebral amyloid angiopathy. Acta Neuropathol. 133 (3), 409–415. doi:10.1007/s00401-016-1635-0.

van Veluw, S.J., Scherlek, A.A., Freeze, W.M., Ter Telgte, A., van der Kouwe, A.J., Bacskai, B.J., Frosch, M.P., Greenberg, S.M., 2019. Different microvascular alterations underlie microbleeds and microinfarcts. Ann. Neurol. 86 (2), 279–292. doi:10.1002/ana.25512.

Wardlaw, J.M., Smith, E.E., Biessels, G.J., Cordonnier, C., Fazekas, F., Frayne, R., Lindley, R.I., O'Brien, J.T., Barkhof, F., Benavente, O.R., Black, S.E., Brayne, C., Breteler, M., Chabriat, H., Decarli, C., de Leeuw, F.E., Doubal, F., Duering, M., Fox, N.C., Greenberg, S., Hachinski, V., Kilimann, I., Mok, V., Oostenbrugge, R., Pantoni, L., Speck, O., Stephan, B.C., Teipel, S., Viswanathan, A., Werring, D., Chen, C., Smith, C., van Buchem, M., Norrving, B., Gorelick, P.B., Dichgans, M.nEuroimaging, S. T. f. R. V. c. o, 2013. Neuroimaging standards for research into small vessel disease and its contribution to ageing and neurodegeneration. Lancet Neurol. 12 (8), 822–838. doi:10.1016/S1474-4422(13)70124-8.

Yates, P.A., Desmond, P.M., Phal, P.M., Steward, C., Szoeke, C., Salvado, O., Ellis, K.A., Martins, R.N., Masters, C.L., Ames, D., Villemagne, V.L., Rowe, C.C., Group, A.R., 2014. Incidence of cerebral microbleeds in preclinical Alzheimer disease. Neurology 82 (14), 1266-1273. doi:10.1212/WNL.0000000000000285.

Youmans, K.L., Tai, L.M., Nwabuisi-Heath, E., Jungbauer, L., Kanekiyo, T., Gan, M., Kim, J., Eimer, W.A., Estus, S., Rebeck, G.W., Weeber, E.J., Bu, G., Yu, C., Ladu, M.J., 2012. APOE4-specific changes in Abeta accumulation in a new transgenic mouse model of Alzheimer disease. J. Biol. Chem. 287 (50), 41774–41786. doi:10.1074/jbc.M112.407957.

Zhang, J.X., Lai, Y.H., Mi, P.Y., Dai, X.L., Zhang, R., Zhang, Z.J., Zhang, S.J., Zhang, X.W., Zhang, X.Y., Yang, B.Y., Cui, D.M., Zhang, C., Zhao, C.Q., Dou, F., 2019. Rescue of cognitive deficits in APP/PS1 mice by accelerating the aggregation of beta-amyloid peptide. Alzheimers Res. Ther. 11 (1), 106. doi:10.1186/s13195-019-0560-6.